

This file has been cleaned of potential threats.

If you confirm that the file is coming from a trusted source, you can send the following SHA-256 hash value to your admin for the original file.

41acb559a9968027f741d7d12058aa8d0f745d64233dd69a1a029c876f7b6e65

To view the reconstructed contents, please SCROLL DOWN to next page.

The text that follows is a PREPRINT.

Please cite as:

dos Santos Junior, U.M., J.F.C. Gonçalves & P.M. Fearnside: 2012. Measuring the impact of flooding on Amazonian trees: photosynthetic response models for ten species flooded by hydroelectric dams. *Trees-Structure and Function*. (published online first 14 Apr. 2012)

doi:10.1007/s00468-012-0788-2

ISSN: 0931-1890 (print version) 1432-2285 (electronic version)

Copyright: Springer Science + Business Media, LLC

The original publication will be available at: <http://www.springer.com>

1 **Measuring the impact of flooding on Amazonian trees:**
2 **photosynthetic response models for ten species flooded by**
3 **hydroelectric dams**

4
5
6 Ulysses Moreira dos Santos Junior^a, José Francisco de Carvalho Gonçalves^{a,*},
7 Philip Martin Fearnside^b

8
9 ^a Laboratório de Fisiologia e Bioquímica Vegetal, Instituto Nacional de Pesquisas da
10 Amazônia (MCT-INPA), Manaus, Amazonas, Brazil Tel.: +55 92 3643-1880.

11 ^b Coordenação de Pesquisas em Ecologia, Instituto Nacional de Pesquisas da Amazônia
12 (MCT-INPA), Manaus, Amazonas, Brazil. Tel.: + 55 92 3643-1822. e-
13 mail:pmfearn@inpa.gov.br

14
15 * Corresponding author: E-mail: jfc@inpa.com.br

16
17 22 January 2012

18 Revised 30 August 2012

19
20

21 **Measuring the impact of flooding on Amazonian trees: photosynthetic response models for ten species** 22 **flooded by hydroelectric dams**

23
24 **Abstract** Increasing areas of Amazonian forest are coming under flood stress due to dam construction and
25 greater variability in river flood levels due to climate change. The physiological responses of Amazonian trees
26 subjected to flooding are important to understanding the consequences of these changes. Irradiance-response
27 curves for photosynthesis obtained from ten tropical tree species growing in flooded areas were used to fit three
28 empirical models. The study was done in floodplains along the Uatumã River, both upstream and downstream of
29 the Balbina Hydroelectric Dam in Brazil's state of Amazonas (01° 55'S; 59° 28' W). Ten species were studied.
30 Models compared were: non-rectangular hyperbola (NRH), rectangular hyperbola (RH) and exponential (EXP).
31 All models were quantitatively adequate for fitting the response of measured data on photosynthesis to irradiance
32 for all ten species in the non-flooding and flooding periods. Considerable variation was found among the model
33 estimates of maximum photosynthesis (P_{nmax}), dark respiration (R_d) and apparent quantum yield of
34 photosynthesis (α). For photosynthesis, the two hyperbolas overestimated P_{nmax} while EXP presented more
35 realistic values. For estimating R_d , RH presented the most realistic values. To avoid unrealistic value estimates of
36 R_d we recommend adding measured R_d values to the regressions. The results suggest that the EXP model
37 presented the most realistic P_{nmax} and α values, and, in spite of less accuracy in fitting photosynthetic irradiance
38 curves than the RH model, it can be recommended for accessing the information used in photosynthetic
39 irradiance curves for the leaves of tropical trees growing in Amazonian floodplains or in areas that are artificially
40 flooded by dams.

41
42 **Keywords** Apparent quantum yield – Carbon - Convexity term - Dark respiration – Global warming -
43 Photosynthesis

44 45 **Introduction**

46
47 The carbon balance of Amazonian forests is a matter of global concern because any significant shift towards gain
48 or loss would translate into climatically significant amounts of atmospheric carbon dioxide (Ometto et al. 2005).
49 Forests gain or lose carbon as a result of a balance between rates of tree growth and recruitment on one side and
50 mortality on the other. These rates are affected by the different stresses to which trees are subjected, such as lack
51 of water, light or nutrients. One underappreciated stress in the context of Amazonian forests is that of flooding
52 (Costa et al. 2009). The increased variability in river flow levels expected to result from projected climate
53 changes indicates future increases in areas subject to flooding. The record-breaking Amazon floods of 2009,
54 which even submerged part of downtown Manaus, offer a harbinger of this (Nobre and Borma 2009). Massive
55 plans for dam building would subject additional forest areas to flood stress: Brazil's 2011-2020 electrical
56 expansion plan (Brazil, MME 2011) calls for building 30 dams in the country's Amazon region by 2020, or one
57 dam every four months. The physiological responses of Amazonian trees to stress from flooding are therefore
58 important to understanding the consequences of these changes.

59 Tropical forests play an important role in regional and global CO₂ fluxes and could contribute up to 50% of
60 total global primary productivity (Grace et al. 2001). Soil fertility differences are believed to explain a gradient
61 of increasing net production from east to west in Amazonia (Malhi et al. 2006). Mature Amazonian forests can
62 act either as sinks or sources, depending on climatic conditions, with droughts such as those during El Niño
63 events resulting in net releases of carbon (Tian et al. 1998, 2000; Saleska et al. 2003; Rice et al. 2004; Davidson
64 et al. 2012). Major Amazonian droughts in 2005 and 2010 caused by warm water in the Atlantic Ocean (rather
65 than El Niño, which is triggered by warm water in the Pacific) dramatically stunted tree growth in the region
66 (Phillips et al. 2009; Lewis et al. 2011). Both of these forms of drought are expected to increase in frequency
67 and severity as a result of global warming (Cox et al. 2004, 2008). On the other hand, a major Amazonian flood
68 occurred during a La Niña event in 2009 that caused excess rainfall in the in the north and northeast of Amazon
69 region (Marengo et al. 2011). Although the effect of drought dominates interannual variation in production in
70 Amazonia as a whole, the effect of flooding is also an important factor in forest productivity.

71 Stress from flooding may play a substantial role in limiting the productivity of Amazonian forest trees.
72 Current estimates indicate a large area of Amazonia that is subject to annual flooding. Traditionally, the
73 annually flooded area in the Brazilian portion of the Amazon has been considered to be 70,000 km², or 2% of
74 Brazil's share of the forest (Goulding 1980). Recently, synthetic-aperture radar (SAR) imagery from the
75 Japanese Earth Resources Satellite (JERS), which can "see" through both clouds and tree cover to detect
76 standing water on the forest floor, has produced much higher estimates, approximately 850,000 km² of forest
77 (i.e., not counting savanna wetlands) being subject to flooding throughout the lowland Amazon in all of the
78 countries that share the basin (Melack et al. 2004). This represents 17% of the forest, or an area more than double
79 that of the US state of California. The areas affected by this "natural" flooding may increase as a result of
80 hydrological impacts from land-use change (Costa et al. 2003) and climate change (Marengo et al. 2009).

81 Trees undergoing flooding stress are believed to halt or greatly reduce their rates of photosynthesis. At two
82 forest sites located approximately 80 km North of Manaus and 100 km from the Balbina Dam, the Large-Scale
83 Biosphere-Atmosphere (LBA) Project has measured CO₂ fluxes above the forest canopy from two 55-m high
84 towers. Significantly lower carbon uptake at one of the two sites was ascribed to the larger area of seasonally
85 flooded “*baixio*” (valley bottom) in the area surrounding the tower (Araújo et al. 2002).

86 The effect of “natural” flooding is now being joined by the effects of hydroelectric dams. Reservoirs
87 fluctuate in water level, and at their peak water levels they temporally flood surrounding forest. Forests that are
88 flooded permanently or for long periods of the year are killed, but those at slightly higher elevations that are only
89 occasionally flooded for short periods will experience stress, killing some trees and slowing the growth of others.
90 The raising of the water table in the forest surrounding the shoreline stresses trees even when pooled water at the
91 surface is not present. For example, in the forest adjacent to the Samuel Reservoir in the state of Rondônia, in
92 southwestern Amazonia, red dots visible on Landsat satellite imagery indicate this stressed forest (see Fearnside
93 2005). The Balbina Dam, where the current study was done, has several thousand km of shoreline, including the
94 perimeters of approximately 3000 islands (e.g., Fearnside 1989). The forested portion of Brazilian Amazonia
95 now has four “large” dams (Curuá-Una, Tucuruí, Balbina and Samuel) and three under construction (Belo
96 Monte, Santo Antônio and Jirau). The only publically available long-range plan, independent of projected
97 construction dates, indicates a total of 79 dams flooding 100,000 km² in Brazilian Amazonia (Brazil
98 ELETROBRÁS 1987; see Fearnside 1995). The scale of these plans means that better tools are needed to assess
99 dam impacts, including the impact of flooding stress on trees. Quantitative information on the effect of flooding
100 on photosynthesis of tree species in these areas has been lacking and is supplied in the present paper for ten
101 species. Identification of the best models for representing these impacts will facilitate future extension of the
102 knowledge base relating flood stress to photosynthesis in tropical forest trees.

103 Several studies have been done to quantify the assimilation and emission of CO₂ by different forest types
104 and by the different species that compose the forest ecosystems (Zhan et al. 2003; Oren et al. 2006; Stoy et al.
105 2006; Mercado et al. 2006). Models of photosynthesis play key roles in estimating primary production of
106 vegetation under different conditions and have been used in ecosystem simulations and ecosystem modeling
107 (Gao et al. 2004; Muraoka and Koizumi 2005). Complex mechanistic models of photosynthesis, such as the
108 biochemical models of Farquhar et al. (1980) for C₃ leaves, have often been applied in studies of photosynthesis
109 mechanisms (Peri et al. 2005). These models are usually derived from known quantitative relationships between
110 different kinds of molecules involved in the biochemical processes of photosynthesis and require rather extensive
111 calibration as well as complex parameterization (Cannell and Thornley 1998). Including a detailed representation
112 of biochemical processes in the biochemical models is not always advantageous, as compared to the simpler leaf-
113 photosynthetic models (Gao et al. 2004).

114 Due the complexity of mechanistic models, empirical models have been used to obtain information from
115 irradiance-response curves of photosynthesis under different conditions (Sullivan et al. 1996; Eschenbach et al.
116 1998; Mielke et al. 2003; Morais 2003; Mielke and Schaffer 2010; Silva et al. 2011). Different models have been
117 observed to produce large differences in estimates of important parameters obtained from photosynthesis-
118 irradiance curves, such as maximum photosynthesis (P_{nmax}), dark respiration (R_d) and the apparent quantum yield
119 of photosynthesis (α). These differences can cause errors in the interpretation of the data.

120 In spite of the differences among the models used in the literature, little attention has been paid to
121 comparison of characteristics and behavior among models for estimating the main photosynthetic parameters.
122 The goal of this study was to investigate the differences in estimates of the main photosynthetic parameters
123 (P_{nmax} , R_d and α) produced by the three traditional models (non-rectangular hyperbola, rectangular hyperbola and
124 exponential) and to analyze the three models by fitting measured data on photosynthesis in ten tropical tree
125 species under flooding and non-flooding conditions.

127 **Material and methods**

129 **Study area and species selection**

131 The study was conducted in floodplains along the Uatumã River, both upstream and downstream of the Balbina
132 hydroelectric dam, located about 220 km from Manaus in Presidente Figueiredo County, Amazonas state, Brazil
133 (01° 55'S; 59° 28' W). The climate at this site is Amw under the Köppen classification system. In the period of
134 the experiment (2005 – 2007) the annual average rainfall was 2392 mm and average values of minimum and
135 maximum temperature were 23.3 and 33.9°C, respectively. Monthly rainfall at the study location was obtained
136 from Manaus Energia, the power company that operates the Balbina Dam. The physiological data were collected
137 in two different periods (flooding and non-flooding). The non-flooding period was characterized by the reservoir
138 water level varying between 47.64 and 48.21 m above mean sea level (January and February of 2006 and 2007)
139 and the flooding period was characterized by the water level varying between 50.41 and 50.69 m (June and July
140 of 2006 and 2007). The measurements of light curves were performed on ten plants for each of seven species

141 tolerant to flooding and for three non-tolerant species. After selection of the species in the field, fertile botanical
142 material was collected for identification in the herbarium of the Instituto Nacional de Pesquisas da Amazônia
143 (INPA). The flood-tolerant species were *Nectandra amazonum* Nees (Lauraceae), *Macrolobium angustifolium*
144 (Benth.) Cowan (Caesalpinaceae), *Alchornea discolor* Klotzch (Euphorbiaceae), *Brosimum lactescens* (S.
145 Moore) C.C. Berg (Moraceae), *Senna reticulata* Willd. (Caesalpinaceae), *Genipa spruceana* Steyererm.
146 (Rubiaceae), *Parinari excelsa* Sabine (Chrysobalanaceae) and the non-tolerant species were *Cecropia concolor*
147 Willd (Cecropiaceae), *Vismia guianensis* (Aubl.) Choisy (Clusiaceae) and *Vismia japurensis* Reichardt
148 (Clusiaceae).

149 150 Photosynthetic measurements

151
152 Measurements of photosynthesis-irradiance (P_n -I) curves (or “light curves”) were performed on healthy,
153 completely expanded leaves in ten plants per species (ten species) in each period (flooding and non-flooding)
154 from 7:30 to 16:30 h using a LI-6400 portable photosynthesis system (Li-cor, USA) equipped with an artificial
155 irradiance source (6400-02B Red Blue). The P_n -I curves were derived using the “light curve” routine in the
156 OPEN 3.4 software modified to accommodate eleven levels of photosynthetic photon flux density (PPFD: 0, 25,
157 50, 75, 100, 250, 500, 750, 1000, 1500, 2000 $\mu\text{mol quanta m}^{-2} \text{s}^{-1}$) in decreasing order. The minimum time
158 allowed for the reading to stabilize at each PPFD level was 120 s, the maximum time for saving each reading
159 was 300 s, and the maximum coefficient of variation (C.V.) was 1%. The Li-cor 6400 was adjusted to a flow rate
160 of 400 $\mu\text{mol s}^{-1}$. The concentration of CO_2 (from a CO_2 cylinder mixed with atmospheric CO_2) was 380 μmol
161 mol^{-1} and the concentration of H_2O vapor inside the assimilation chamber was $21 \pm 3 \text{ mmol mol}^{-1}$. Block
162 temperature was $31 \pm 1^\circ\text{C}$. Before each measurement the leaves were exposed to 1000 $\mu\text{mol (quanta) m}^{-2} \text{s}^{-1}$ for
163 an adaptation period of 5 to 10 min, after which the measurements of the P_n -I curves were performed.

164 165 Description of the models

166
167 Three empirical models were tested: (1) Non-rectangular hyperbola (Marshall and Biscoe, 1980), (2) Rectangular
168 hyperbola (Thornley 1976) and (3) Exponential (Iqbal et al. 1997) (Table 1).

169 In the models: I is the irradiance (\sim PPFD); P_n is the rate of net photosynthesis ($\mu\text{mol CO}_2 \text{ m}^{-2} \text{ s}^{-1}$); $P_{n\text{max}}$ is
170 the maximum photosynthesis; R_d is dark respiration ($\mu\text{mol CO}_2 \text{ m}^{-2} \text{ s}^{-1}$) corresponding to the value of P_n when $I =$
171 $0 \mu\text{mol m}^{-2} \text{ s}^{-1}$; θ is a dimensionless convexity term, and α is the apparent quantum yield of photosynthesis (mol
172 $\text{CO}_2 \text{ mol quanta}^{-1}$).

173 A non-rectangular hyperbola (NRH) was fitted according to Model 1 (Table 1). To avoid correlation
174 between α and θ during curve fitting, α was first found by least-squares regression of the initial linear portion of
175 curve, including darkness (PPFD between 0-100 $\mu\text{mol m}^{-2} \text{ s}^{-1}$). The result of the Kok effect in estimates of α was
176 analyzed in this study. For rectangular hyperbolas and exponential models α was estimated with the non-linear
177 curves.

178 In this study two situations were analyzed. In the first the estimated parameters were R_d , $P_{n\text{max}}$ and α or θ ,
179 depending of the model used. In the second a measured dark respiration (R_d) term was added to the model and
180 only $P_{n\text{max}}$ and α or θ were estimated by the models. The “measured” α was estimated by linear regression of P_n
181 on PPFD between 0-100 $\mu\text{mol m}^{-2} \text{ s}^{-1}$; the measured R_d was considered to be the value of CO_2 flux when when
182 PPFD = 0 $\mu\text{mol m}^{-2} \text{ s}^{-1}$, and the measured $P_{n\text{max}}$ was considered to be the mean value of P_n when PPFD ≥ 1500
183 $\mu\text{mol m}^{-2} \text{ s}^{-1}$.

184 185 Statistical analysis

186
187 Every model was fitted to measured data from each of the 200 P-I curves using the Levenberg-Marquardt
188 algorithm in the non-linear least-squares estimation routine in the Statistica for Windows (Version 6.0) software
189 (StatSoft Inc., Tulsa, OK, USA). The initial values for $P_{n\text{max}}$, R_d , α and θ were set at 10 $\mu\text{mol CO}_2 \text{ m}^{-2} \text{ s}^{-1}$, 0.1
190 $\mu\text{mol CO}_2 \text{ m}^{-2} \text{ s}^{-1}$, 0.01 $\text{mol CO}_2 \text{ mol}^{-1}$ photons and 0.1, respectively, making them coherent with the predicted
191 values. None of the initial values for $P_{n\text{max}}$, R_d , α and θ were modified.

192 For each model, the goodness of fit was verified by plotting the modeled curve against the mean of ten
193 measured curves for each species, based on the analysis of residuals, the coefficient of determination (r^2), the
194 average of unsigned deviation (*Aud*) and the root mean square of error (*RMSE*). The r^2 value was used to
195 evaluate the amount of variation explained by a regression; this statistic is commonly used to select the best
196 regression. Due the r^2 giving heavy weight to observations with large magnitudes, an additional loss function was
197 used to verify the best fit: average of unsigned deviation ($Aud\% = \Sigma (|(Predicted-measured)|/measured) \times 100/n$).
198 As an alternative statistic to confirm the best goodness of fit for the models, the root mean square error (*RMSE*),
199 or $\sqrt{\Sigma \text{Error}^2/n}$, was reported.

200

Results

Comparison of the fits and of the estimates of P_{nmax} , R_d , α and θ produced by the models

All three models were adequate ($P < 0.013$ for all species in the two periods) and showed high coefficients of determination ($r^2 > 0.94$) for all species in both the non-flooding (NFP) and flooding (FP) periods (Table 2). Comparing the goodness of fit of the models, RH generally had the best fit as shown by the lower values of average unsigned deviation (*Aud%*) and root mean square error (*RMSE*) for all of the species studied (Table 2). NRH produced the worse fit.

The three models showed a random distribution of residuals around the predicted values for all species in both periods (Fig. 1). The RH model presented the lowest values of residuals for all levels of PPFD, as compared to the NRH and EXP models (Fig. 1). In general, the NRH and EXP models presented an underestimation of P_n at PPFD = 0, 25, 500, 750 and 1000 $\mu\text{mol m}^{-2} \text{s}^{-1}$ and an overestimation of P_n at PPFD = 50, 75, 100, 250, 1500 and 2000 $\mu\text{mol m}^{-2} \text{s}^{-1}$ (Fig. 1).

In Fig. 2 estimates of maximum net photosynthesis (P_{nmax}), predicted dark respiration (R_d) and predicted apparent quantum yield of photosynthesis (α) as calculated by the models are plotted against the measured values for 200 plants from ten species and two periods (non-flooding and flooding). The best estimate of P_{nmax} was presented by the EXP model while the two hyperbolas overestimated the values of P_{nmax} (Fig. 2A-B; Table 3). NRH exhibited values of predicted P_{nmax} higher than measured P_{nmax} , varying, depending on the species, from 33.7 to 80.5% (NFP) and from 7.3 to 62.4% (FP). RH presented values of P_{nmax} that were higher than the measured P_{nmax} by 11 to 31.1% (NFP) and by 5.2 to 36.9% (FP) (Table 3). On the other hand, the EXP model presented good estimates of P_{nmax} for all species, presenting a slight underestimation. In addition, EXP showed the best correlation between measured and predicted values of P_{nmax} , while NRH showed the worse. For R_d RH presented a good estimate, with mean overestimates of 5.8% (NFP) and 9.9% (FP) for all species (Table 4). On the other hand, NRH and EXP exhibited a clear underestimation of R_d . In addition, all of the models showed negative values of predicted R_d , indicating problems for interpretation of these data (Fig. 2C-D).

The α value estimated by linear regressions with exclusion of points from the Kok-effect region (PPFD < 20 $\mu\text{mol m}^{-2} \text{s}^{-1}$) had mean underestimations of 7.6% (NFP) and 8.9% (FP) as compared to measured α (PPFD 0-100 $\mu\text{mol m}^{-2} \text{s}^{-1}$) (Table 5). The α estimated by the RH models was, on average, 43.8 (NFP) and 70.0% (FP) higher than the measured α , and for the EXP models the estimated values of α underestimated by 1.2% for the flooding period and overestimated by 13.8% for the non-flooding period compared to measured α values, considering all species (Table 5).

Comparison of the fits and of the estimate P_{nmax} , α and θ by the models when R_d values from measured data were added to the models.

When the measured data on R_d were added to the models for estimation of P_{nmax} and α , the accuracy for all models decreased as compared to the models in which estimated values of R_d were used, as demonstrated by decreasing r^2 values and increasing *RMSE* values (compare the values in Tables 2 to 6). However, the models were adequate ($P < 0.01$ for all species and both periods) in the models in which R_d values were estimated.

The analyses of residuals showed higher values than the residuals from the models in which R_d was estimated, especially for NRH (Fig. 3). The RH model continued showing the lowest values for residuals for all levels of PPFD (Fig. 3). The distribution of the residuals showed that the NRH and EXP models overestimated P_n at PPFD = 25 $\mu\text{mol m}^{-2} \text{s}^{-1}$, while the models in which R_d was estimated presented an underestimates (Compare Fig. 3 to Fig. 1).

In Fig. 4, estimates of maximum net photosynthesis (P_{nmax}) and predicted apparent quantum yield of photosynthesis (α) when R_d was added to the models (as calculated by the models) are plotted against the measured for 200 plants from ten species and two periods (non-flooding and flooding). For the estimated parameters a better estimation of P_{nmax} by NRH was found when R_d was added, as compared to the situation in which R_d was estimated by the NRH model (Compare values of Table 7 to Table 3). For the RH and EXP models a slight difference was observed, in which the EXP model showed more realistic estimates of P_{nmax} , as compared to the two hyperbola models. For α , RH and EXP models presented better linear correlations between measured and estimated values of α , with higher values of r^2 when measured R_d was included in the models (Table 8). In addition, EXP models presented more realistic estimates of α as compared to RH models. For θ in NRH models, on average, underestimates of 7.0% (NFP) and 4.5% (FP) were observed when measured R_d was added to the models, considering all species (Table 9).

Discussion

Models fit performance

261 In this study all three models were quantitatively adequate ($P < 0.013$) in predicting the behavior of the
262 photosynthesis irradiance curves for each species in each period. Similar results were found by Gomes et al.
263 (2006), in which NHR, RH and EXP models were found to be quantitatively adequate for dwarf coconut. To
264 evaluate the best quantitative performance among the three models the values of r^2 , $Aud\%$ and $RMSE$ were
265 observed. Higher values of r^2 and lower values of $Aud\%$ and $RMSE$ for RH may indicate better accuracy and
266 quantitative performance compared to the other two models for the majority of the species studied in the two
267 periods, especially for NRH models. Some studies have used the F -test to compare the variability of predictions
268 with the variability of measured data with lower absolute values of F indicate better quantitative performance
269 (Patchesky et al. 1996; Gomes et al. 2006). Using the F -test, Gomes et al. (2006) concluded that EXP models had
270 better quantitative performance than the two hyperbolas.

271 Analyses of residuals confirmed the results shown by the $Aud\%$ and $RMSE$ values, indicating that RH model
272 presented the better goodness of fit than EXP and NRH models. On the other hand, NHR model showed the
273 highest residuals around the predicted values of P_n , except for *C. concolor* in the non-flooding period (Fig 1). For
274 *S. reticulata* (NFP and FP) and *C. concolor* (NFP), the high values of residuals may be the result of the high
275 values of P_n that these species exhibited. It is interesting to observe that in some PPFd for some species the
276 behavior of residuals for RH was different from the NHR and EXP models. Therefore, while RH models showed
277 an overestimation of residual values, NHR and EXP models showed underestimations of the values of residuals
278 (see *N. amazonum*, *G. spruceana*, Fig. 1).

279 P_{nmax} performance

281 Estimates of P_{nmax} varied depending on the model used. The best estimation was presented by the EXP
282 model, while NRH and RH models resulted in large overestimations. A similar result was found by Gomes et al.
283 (2006), who concluded that P_{nmax} was more realistic when estimated by the EXP model. The good estimation of
284 P_{nmax} by the EXP model suggests that this empirical model can be used as a submodel for predicting values in
285 productivity models and for environmental modeling of the CO_2 balance.

286 R_d performance - part 1

288 The most realistic estimation of R_d was obtained from the RH model, while the EXP and NRH models
289 presented a high underestimates. The underestimation of R_d can be substantial, as observed in this study for some
290 plants, and the estimated values can be unrealistic (see Fig. 2C-D), with the estimates of R_d values reaching
291 negative values (for the models, R_d present positive values). Similar results were found by Vervuren et al.
292 (1999), who observed that R_d was negative in some cases, suggesting unrealistic estimates of respiratory oxygen
293 production. This fact can be problematic for the interpretation and comprehension of the CO_2 balance in single
294 plants and even more so for vegetation.

295 α performance

297 The calculation of α varied among the three models tested. First the Kok-effect region was analyzed in the
298 estimation of α . The α value is estimated from the initial slope of the linear regression of the $P_n - I$ curves, where
299 the net photosynthesis is linear with increasing irradiance. In this study, exclusion of points from the Kok effect
300 region (Sharp et al., 1984) was found to promote, on average, an underestimation of 7.6% (NFP) and 8.9% (FP)
301 of α as compared to the α estimated from initial slope including points in the Kok-effect region (e.g., PPFd = 0
302 $\mu\text{mol m}^{-2} \text{s}^{-1}$). Similar results were observed by Clearwater et al. (1999) and Gonçalves and Santos Junior (2005),
303 who found differences of 10 and 12.5%, respectively. According Leverenz (1987), this difference occurs due to
304 increases in mitochondrial respiration at very low irradiance (PPFD < 20 $\mu\text{mol m}^{-2} \text{s}^{-1}$). The inclusion of the
305 points from the Kok-effect region is responsible for increasing the angular coefficient (slope) of the linear
306 regression from the initial slope and, consequentially, increasing the α values.

307 When α was estimated by the RH model a substantial overestimation was observed as compared to measured
308 α values (or linearly estimated from PPFd ~ 0-100 $\mu\text{mol m}^{-2} \text{s}^{-1}$). This overestimation by RH has been
309 demonstrated in many studies (Mielke et al. 2003; Gomes et al. 2006). In addition, Hootsman and Vermaat
310 (1991) found a satisfactory goodness of fit for the RH model, however, on the basis of the consistent parameter
311 overestimation of P_{nmax} and α as observed by Vervuren et al. (1999) and Iwakuma and Yasuno (1983),
312 application of the RH model was considered inappropriate by these authors. For the EXP model substantial
313 overestimation of α was found, on average, for the species in the flooding period, especially for *C. concolor*, *V.*
314 *guianensis* and *V. japorensis*, that presented low values of α . These results indicated that the RH and EXP
315 models presented higher overestimation for low values of α . The linear correlation between α values estimated
316 by RH and EXP models for all species together was higher ($r^2 > 0.92$, data not shown) as compared to the
317 correlation between measured α values and α values estimated by the RH model ($r^2 > 0.57$) and the EXP model
318 ($r^2 > 0.647$) (see Table 4), indicating that the principles for calculating α by RH and EXP models are similar.

319 Theoretically, the maximum value that α can reach is 0.125 mol mol^{-1} , meaning that 8 moles of photons are
320 required to reduce 1 mole of CO_2 in the absence of photorespiration (Singsaas et al. 2001). However, due to

321 cyclic photophosphorylation, the maximum α value may be closer to 0.112 in most C_3 plants). Comparing the
322 estimating α by the models, RH model presented values closer to the theoretical maximum α . However, the α
323 values estimated by the models were much lower than the theoretical maximum. These results have been found
324 by many researchers in the context of a large set experiments with many different species, with reported values
325 30-85% lower than the $0.125 \text{ mol mol}^{-1}$ theoretical maximum (Clearwater et al. 1999, Marengo et al. 2001a,b;
326 Singaas et al. 2001; Santos Junior 2003; Gonçalves et al, 2005). The low values of α may be the result of
327 unfavorable environmental factors (e.g. drought, flooding, high irradiance) and/or may originate from
328 physiological processes that compete with CO_2 reduction, such as photoinhibition that provokes damage to the
329 photosynthetic apparatus (Groom and Baker 1992; Gonçalves et al. 2005), photorespiration (Sharkey 1988;
330 Peterson 1990; Singaas et al. 2001) and alternative competitors such as NO_3^- and oxygen reduction outside of
331 the photorespiration process (Edwards and Walker 1983; Robinson 1988; Cornic and Briantais 1991).

332 Thus, for estimates of α , all models are adequate. However, one must avoid comparing values of α
333 calculated by different models; in other words, when researchers compare their results to those of others they
334 must pay close attention to how the α values were estimated.

335 *R_d performance - part 2*

336 To avoid problems in estimation of R_d (see discussion above), measured R_d values were included in the
337 models and only P_{nmax} and α or θ were estimated by the models. This solution has been used by some researchers
338 to avoid problems with the underestimation of R_d (Clearwater et al. 1999; Vervuren et al. 1999; Gonçalves et al.
339 2005). When R_d was included in the models the regressions, on average, lose accuracy as compared to the
340 situation in which R_d was estimated, as indicated by the decrease of r^2 values and the increase of *Aud*% (except
341 for RH models in the non-flooding period) and *RMSE*. The loss of accuracy was most evident in the NRH model.
342 This result was confirmed by the analysis of residuals in which the NRH model presented higher values of
343 residuals as compared to the RH and EXP models. This indicates that use of the NRH model may provoke much
344 more error in modeling the photosynthetic irradiance response than the RH and EXP models. In addition, it is
345 clear that, in spite of NRH having been frequently used by many researchers, for the species in this study its
346 presented the worse quantitative performance, as compared to the RH and EXP models.

347 For estimation of P_{nmax} , the EXP models continued presenting the most realistic estimates as compared to the
348 two hyperbolic models, suggesting that the EXP models are most adequate for estimating P_{nmax} in both situations.
349 EXP also presented better estimates for α than did the RH models. These results suggest that the main problem
350 presented by the EXP model is in estimating R_d , because for P_{nmax} and α , the EXP model presented the best
351 estimation.

352 *Convexity term (θ) performance in non-rectangular hyperbola*

353 For estimating the convexity term (θ), mean values of 0.838 (NFP) and 0.884 (FP) were observed (Table 9).
354 When measured values of R_d were added to the models, the estimated θ increased, on average, by 7.0 and 4.5%
355 for the non-flooding and flooding periods, respectively. These results were higher than the θ values observed by
356 Thomas and Bazzaz (1999) in a study of dipterocarp species (θ value ranging from 0.20 to 0.80). On the other
357 hand, Santos Junior (2003) and Gonçalves et al. (2005) found values of θ ranging from 0.85 to 0.97 for tree
358 species in Amazonian forest. The low and high values of θ are related to gradual and abrupt transitions,
359 respectively, in the light curve, between the region where irradiance is limiting and the region where irradiance is
360 saturated (Thornley 1998). The convexity term has been related to irradiance saturation in chloroplasts, and
361 factors such as irradiance, stress conditions, pigment content and foliar morphology may affect the θ value
362 (Leverens 1987; Hirose and Werger 1987; Evans 1993; Ogren 1993; Kull and Niinementes 1998).

363 **Conclusions**

364 In this study all three models were quantitatively adequate for fitting the response of measured data of
365 photosynthesis to irradiance, in all ten species in the non-flooding and flooding periods. However, RH and EXP
366 were more adequate than NRH in both situations in which R_d was estimated or in which the measured R_d was
367 added to the regression. For parameter estimation, considerable variation was found among estimates of P_{nmax} , R_d
368 and α among the models. These differences must be considered in the interpreting the data and in making
369 comparisons with the results of other researchers. For photosynthesis, the two hyperbolas overestimate P_{nmax}
370 while EXP presented more realistic values. Considering the estimation of R_d , the RH model presented the most
371 realistic values, as compared to the NRH and EXP models. However, all models presented problems to estimate
372 R_d , because for any plants the estimated values were biologically impossible to explain. To avoid this situation,
373 especially for the NRH and EXP models, the solution is to add the measured R_d term to the regression. When the
374 R_d term was added, EXP presented the most realistic estimation of P_{nmax} and α , as compared to the RH, and NRH
375 models, which continued to overestimate P_{nmax} . Thus, we conclude that: a) R_d should be added to the regressions
376 to avoid problems of unrealistic estimated values of R_d ; b) The NRH model, in spite of being frequently used,

381 was less accurate in fitting the photosynthetic irradiance-curves and performed poorly in estimating P_{nmax} , as
382 compared to the RH and EXP models; c) The RH model presented the best accuracy to fitting the photosynthetic
383 irradiance-curves and can be recommended for adjusting the light curves. However, the RH models presented
384 problems to overestimated P_{nmax} and α ; d). The EXP model presented most realistic P_{nmax} and α values and, in
385 spite of showing less accuracy in fitting photosynthetic-irradiance curves than the RH model, this model can be
386 recommended for accessing photosynthetic irradiance curves for the leaves of tropical trees growing in Amazon
387 floodplains or in artificially flooded areas, such as dams. These curves constitute a key tool for understanding the
388 impact of flooding on carbon balance in Amazonian forests that are being increasingly subjected to stress from
389 flooding.

390 Acknowledgements

391 We thank the Conselho Nacional de Desenvolvimento Científico e Tecnológico (CNPq); the Fundação de
392 Amparo à Pesquisa do Estado do Amazonas (FAPEAM), the Large-Scale Atmosphere-Biosphere Experiment in
393 Amazonia (LBA), the Instituto Chico Mendes (ICMBio), the Manaus Energia, The IBAMA and the entire team
394 of the Laboratory of Plant Physiology and Biochemistry. J.F.C Gonçalves and P.M. Fearnside acknowledge
395 fellowships provided by CNPq.

396 References

- 397 Araújo AC, Nobre AD, Kruijt B, Dallarosa R, Elbers J, Stefani P, Von Randow C, Manzi AO, Gash JHC, Kabat
398 P (2002) Comparative measurements of CO₂ exchange for two towers in an Amazonian rainforest: The
399 LBA Manaus site. *Journal of Geophysical Research* 107(D20) doi: 10.1029/2001JD000676
400 Brazil, ELETROBRÁS (1987) Plano 2010: Relatório Geral. Plano Nacional de Energia Elétrica 1987/2010
401 (Dezembro de 1987). Centrais Elétricas do Brasil (ELETROBRÁS), Brasília, DF, Brazil. 269 pp.
402 Brazil, MME (2011) Plano Decenal de Expansão de Energia 2020. MME (Ministério de Minas e Energia),
403 Empresa de Pesquisa Energética. Brasília, DF, Brazil. 2 vols.
404 Cannell MGR, Thornley JHM (1998) Temperature and CO₂ responses of leaf and canopy photosynthesis: a
405 clarification using the non-rectangular hyperbola model of photosynthesis. *Ann Bot* 82:883-892
406 Clearwater MJ, Susilawaty R, Efendi R, Gardingen PR (1999) Rapid photosynthetic acclimation of *Shorea*
407 *johorensis* seedlings after logging disturbance in Central Kalimantan. *Oecologia* 121:478-488.
408 Cornic G, Briantais J (1991) Partitioning of photosynthetic electron flow between CO₂ and O₂ reduction in a C₃
409 leaf (*Phaseolus vulgaris* L.) at different CO₂ concentration and during drought stress. *Planta* 183:178-
410 184.
411 Costa MH, Botta A, Cardille JA (2003) Effects of large-scale changes in land cover on the discharge of the
412 Tocantins River, southeastern Amazonia. *Journal of Hydrology* 283:206-217.
413 Costa, MH, Coe, MT, Guyot, JL (2009) Effects of climatic variability and deforestation on surface water
414 regimes. In: Keller M, Bustamante M, Gash J, da Silva Dias P (Eds.), Amazonia and Global Change.
415 Geophysical Monograph Series, Volume 186, American Geophysical Union (AGU), Washington, DC,
416 U.S.A., pp. 543-553.
417 Cox PM, Betts RA, Collins M, Harris PP, Huntingford C, Jones CD (2004) Amazonian forest dieback under
418 climate-carbon cycle projections for the 21st century. *Theor Appl Climatol* 78:137-156.
419 Cox PM, Harris PP, Huntingford C, Betts RA, Collins M, Jones CD, Jupp TE, Marengo JA, Nobre CA (2008)
420 Increasing risk of Amazonian drought due to decreasing aerosol pollution. *Nature* 453:212-215.
421 Davidson EA, Araújo AC, Artaxo P, Balch JK, Brown JF, Bustamante MMC, Coe MT, Defries RS, Keller M,
422 Longo M, Munger JW, Schroeder W, Soares-Filho BS, Souza Jr CM, Wofsy SC (2012) The Amazon
423 Basin in Transition. *Nature* 481:321-328
424 Edwards E, Walker D (1983) C₃, C₄: mechanisms, and cellular and environmental regulation, of photosynthesis.
425 Blackwell, Oxford.
426 Evans JR (1993) Photosynthetic acclimation and nitrogen partitioning within theoretical optimum. *Aust J Plant*
427 *Physiol* 20:69-82.
428 Eschenbach C, Glauner R, Kleine M, Kappen L (1998) Photosynthesis rates of selected tree species in lowland
429 dipterocarp rainforest of Sabah, Malaysia. *Trees* 12:356-365.
430 Farquhar GD, von Caemmerer S, Berry JA (1980) A biochemical model of the photosynthetic CO₂ assimilation
431 in leaves of C₃ species. *Planta* 149:78-90.
432 Fearnside PM (1989) Brazil's Balbina Dam: Environment versus the legacy of the pharaohs in Amazonia.
433 *Environmental Management* 13:401-423.
434 Fearnside PM (1995) Hydroelectric dams in the Brazilian Amazon as sources of 'greenhouse' gases.
435 *Environmental Conservation* 22:7-19.
436 Fearnside PM (2005). Brazil's Samuel Dam: Lessons for hydroelectric development policy and the environment in
437 Amazonia. *Environmental Management* 35:1-19.

- 441 Gao Q, Zhang X, Huang Y, Xu H (2004) A comparative analyses of four models of photosynthesis for 11 plant
442 species in the Loess Plateau. *Agricultural and Forest Meteorology* 126:203-222.
- 443 Gomes FP, Oliva MA, Mielke MS, Almeida A-AF, Leite HG (2006) Photosynthetic irradiance-response in
444 leaves of dwarf coconut palm (*Cocos nucifera* L. "nana", Araceae): Comparison of three models.
445 *Scientia Horticulture* 109:101-105.
- 446 Gonçalves JFC, Barreto DCS, Santos Junior UM, Fernandes AV, Sampaio PTB, Buckeridge MS (2005) Growth,
447 photosynthesis and stress indicators in young rosewood plants (*Aniba rosaeodora* Ducke) under
448 different light intensities. *Braz J Plant Physiol* 17:325-334.
- 449 Gonçalves JFC, Santos Junior UM (2005) Assimilação de carbono e indicadores de estresse da Amazônia. In:
450 Nogueira, RJMC, Araújo EL, Willadino LG, Cavalcante, UMT (Ed). *Estresses ambientais: danos e*
451 *benefícios em plantas*. Recife: UFRPE, Imprensa Universitária; p. 500 (Chapter 15:165-181 ISBN 85-
452 87459-20-1).
- 453 Goulding M (1980) *The Fishes and the Forest: Explorations in Amazonian Natural History*. University of
454 California Press, Berkeley, 280 pp.
- 455 Grace J, Malhi Y, Higuchi N, Meir P (2001) Productivity and carbon fluxes of tropical rain forest. In: Roy HAM
456 (Ed). *Global Terrestrial Productivity*. Academic Press, San Diego.
- 457 Groom QJ, Baker NR (1992) Analysis of light-induced depressions of photosynthesis in leaves of a wheat crop
458 during the winter. *Plant Physiol* 100:1217-1223.
- 459 Hirose T, Werger MJA (1987) Nitrogen use efficiency in instantaneous and daily photosynthesis of leaves in
460 canopy of a *Solidago altissima* stand. *Physiol Plant* 70:215-222.
- 461 Hootsman MJM, Vermaat JE (1991) Light-response curves of *Potamogeton pectinatus* L. as a function of plant
462 age and irradiance level during growth. In *Macrophytes, a key to understanding changes caused by*
463 *eutrophication in shallow freshwater ecosystems*. pp. 57-130. PhD Thesis. International Institute for
464 Hydraulic and Environmental Engineering. Delft.
- 465 Iqbal RM, Rao A-R, Rasul E, Wahid A (1997) Mathematical models and response functions in photosynthesis:
466 an exponential model. In: Pessarakli M. (Ed.), *Handbook of photosynthesis*. Marcel Dekker Inc., New
467 York, U.S.A., pp. 803–810.
- 468 Iwakuma T, Yasuno M (1983) A comparison of several mathematical equations describing photosynthesis-light
469 curve for natural phytoplankton population. *Archiv fur Hydrobiologie* 97:208-226.
- 470 Kull O, Niinemets U (1998) Distribution of leaf photosynthetic properties in tree canopies: comparison of
471 species with different shade tolerance. *Funct Ecol* 12:472-479.
- 472 Leverenz JW (1987) Chlorophyll content and the light response curve of shade-adapted conifer needles. *Physiol*
473 *Plant* 71:20-29.
- 474 Lewis SL, Brando PM, Phillips OL, van der Heijden GMF, Nepstad D (2011) The 2010 Amazon drought.
475 *Science* 331:554.
- 476 Malhi Y, Wood D, Baker TR, Wright J, Phillips OL, Cochrane T, Meir P, Chave J, Almeida S, Arroyo L,
477 Higuchi N, Killeen T, Laurance SG, Laurance WF, Lewis SL, Monteagudo A, Neill DA, Vargas PN,
478 Pitman NCA, Quesada CA, Salomão R, Silva JNM, Lezama AT, Terborgh J, Martínez RV, Vinceti B
479 (2006) The regional variation of aboveground live biomass in old-growth Amazonian forests. *Global*
480 *Change Biol* 12:1107-1138.
- 481 Marengo RA, Gonçalves JFC, Vieira G (2001a). Leaf gas exchange and carbohydrates in tropical trees differing
482 in successional status in two light environments in central Amazonia. *Tree Physiol* 21:1311-1318.
- 483 Marengo RA, Gonçalves JFC, Vieira G (2001b) Photosynthesis and leaf nutrient contents in *Ochroma*
484 *pyramidale* (Bombacaceae). *Photosynthetica* 39:539-543.
- 485 Marengo JA, Jones R, Alves LM, Valverde MC (2009) Future change of temperature and precipitation extremes
486 in South America as derived from the PRECIS regional climate modeling system. *International Journal*
487 *of Climatology* 30:1-15.
- 488 Marengo JA, Tomasella J, Soares WR, Alves LM, Nobre CA (2011) Extreme climatic events in Amazon basin:
489 Climatological and hydrological context of recent floods. *Theor Appl Climatol* DOI 10.1007/s00704-
490 011-0465-1.
- 491 Marshall B, Biscoe PV (1980) A model for C₃ leaves describing the dependence of net photosynthesis on
492 irradiance. *J Exp Bot* 31:29–39.
- 493 Melack JM, Hess LL, Gastil M, Forsberg BR, Hamilton SK, Lima IBT, Novo EMLM (2004) Regionalization of
494 methane emissions in the Amazon Basin with microwave remote sensing. *Global Change Biol* 10:530-544.
- 495 Mercado L, Lloyd J, Carswell F, Malhi Y, Meir P, Nobre AD (2006) Modelling Amazonian forest eddy
496 covariance data: a comparison of big leaf versus sun/shade models for C-14 tower at Manaus I. Canopy
497 photosynthesis. *Acta Amazonica* 36:69-82.
- 498 Mielke MS, Schaffer B (2010) Leaf gas exchange, chlorophyll fluorescence and pigment indexes of *Eugenia*
499 *uniflora* L. in response to changes in light intensity and soil flooding. *Tree Physiol* 30:45-55.

500 Mielke MS, Almeida A-AF, Gomes FP, Aguilar MAG, Mangabeira PAO (2003) Leaf gas exchange, chlorophyll
501 fluorescence and growth responses of *Genipa americana* seedlings to soil flooding. *Environ Exp Bot*
502 50:221-231.

503 Morais RR (2003) *Ecofisiologia de espécies arbóreas crescidas sob condições de plantios na Amazônia central.*
504 Manaus, INPA/UFAM, 158 p.

505 Muraoka H, Koizumi H (2005) Photosynthetic and structural characteristics of canopy and shrub trees in a cool-
506 temperate deciduous broadleaved forest: Implication to ecosystem carbon gain. *Agricultural and Forest*
507 *Meteorology* 134:39-59.

508 Nobre CA, Borma LS (2009) 'Tipping points' for the Amazon forest. *Current Opinion in Environmental*
509 *Sustainability* 1:28-36. Doi:10.1016/j.cosust.2009.07.003.

510 Ogren E (1993) Convexity of the photosynthetic irradiance-response curve in relation to intensity and direction
511 of irradiance during growth. *Plant Physiol* 101:1013-1019.

512 Ometto JP, Nobre AD, Rocha H, Artaxo P, Martinelli L (2005) Amazônia and the modern carbon cycle: Lessons
513 learned. *Oecologia* 143:483-500.

514 Oren R, Hsieh CI, Stoy PC, Albertson J, McCarthy HR, Harrell P, Katul GG (2006) Estimating the uncertainty
515 in annual net ecosystem carbon exchange: spatial variation in turbulent fluxes and sampling errors in
516 eddy-covariance measurements. *Global Change Biol* 12:883-896.

517 Patchesky LB, Hesketh JD, Acock B (1996) An adequate model of photosynthesis I. Parameterization, validation
518 and comparison of models. *Agric Syst* 50:209-225.

519 Peri PL, Moote DJ, McNeil DL (2005) Modelling photosynthetic efficiency (α) for the light-response curve of
520 cocksfoot leaves grown under temperate field conditions. *Eur J Agron* 22:277-292.

521 Peterson RB (1990) Effects of irradiance on the in vivo CO₂:O₂ specificity factor in tobacco using simultaneous
522 gas exchange and fluorescence techniques. *Plant Physiol* 94:892-898.

523 Phillips OL, and 65 others (2009) Drought sensitivity of the Amazon rainforest. *Science* 323:1344-1347.

524 Rice AH, Pyle EH, Saleska SR, Hutyrá L, Palace M, Keller M, de Camargo PB, Portilho K, Marques DF, Wofsy
525 SC (2004) Carbon balance and vegetation dynamics in an old-growth Amazonian forest. *Ecological*
526 *Applications* 14 Supplement: S55-S71.

527 Robinson J (1988) Does O₂ photoreduction occur within chloroplasts in vivo? *Physiol Plant* 72:666-680.

528 Saleska SR, Miller SD, Matross DM, Goulden M, Wofsy SC, da Rocha HR, de Camargo PB, Crill P, Daube BC,
529 de Freitas HC, Hutyrá L, Keller M, Kirchoff V, Menton M, Munger JW, Pyle EH, Rice AH, Silva H
530 (2003). Carbon in Amazon forests: Unexpected seasonal fluxes and disturbance-induced losses. *Science*
531 302:1554-1557

532 Santos Junior UM (2003) *Ecofisiologia de espécies arbóreas plantadas sobre área degradada por atividade*
533 *petrolífera na Amazônia Central.* INPA/UFAM, Manaus, Amazonas, 135 pp.

534 Sharkey TD (1988) Estimating the rate of photorespiration in leaves. *Physiol Plant* 73:666-680.

535 Sharp RE, Mathews MA, Boyer JS (1984) Kok effect and the quantum yield of photosynthesis: light partially
536 inhibits dark respiration. *Plant Physiol* 75:95-101.

537 Singsaas EL, Ort DR, DeLucia EH (2001) Variation in measured values of photosynthetic quantum yield in
538 ecophysiological studies. *Oecologia* 128:15-23.

539 Silva CEM, Gonçalves JFC, Alves EG (2011) Photosynthetic traits and water use species growing on abandoned
540 pasture in different periods of precipitation in Amazonia. *Photosynthetica* 49:246-252.

541 Stoy PC, Katul GG, Siqueira MBS, Juang J-Y, Novick KA, Uebelherr JM, Oren R (2006) *Agricultural and*
542 *Forest Meteorology* 141:2-18.

543 Sullivan NH, Bolstad PV, Vose JM (1996) Estimates of net photosynthetic parameters for twelve tree species in
544 mature forests of the southern Appalachians. *Tree Physiol* 16:397-406.

545 Thomas SC, Bazzaz FA (1999) Asymptotic height as predictor of photosynthetic characteristics in Malaysian
546 rain forest trees. *Ecology* 80:1607-1622.

547 Thornley JHM (1976) *Mathematical models in plant physiology, A quantitative approach to problems in plant*
548 *and crop physiology.* Academic Press, London.

549 Thornley JHM (1998) Dynamic model of leaf photosynthesis with acclimation to light and nitrogen. *Annals of*
550 *Botany* 81:421-430.

551 Tian HQ, Melillo JM, Kicklighter DW, McGuire AD, Helfrich JVK III, Moore, BIII, Vörösmarty CJ (1998)
552 Effect of interannual climate variability on carbon storage in Amazonian ecosystems. *Nature* 396:664-
553 667.

554 Tian HQ, Melillo JM, Kicklighter DW, McGuire AD, Helfrich III J, Moore III B, Vorosmarty CJ (2000)
555 Climatic and biotic controls on annual carbon storage in Amazonian ecosystems. *Global Ecology and*
556 *Biogeography* 9:315-335.

557 Vervuren PJA, Beurskens SMJH, Blom CWPM (1999) Light acclimation, CO₂ response and long-term capacity
558 of underwater photosynthesis in three terrestrial plant species. *Plant Cell Environ* 22:959-968.

559 Zhan X, Xue Y, Collatz GJ (2003) An analytical approach for estimating CO₂ and heat fluxes over the
560 Amazonian region. *Ecological Modelling* 162:97-117.

561
562 **LEGENDS**

563
564 **Figure 1.** Residuals (measured minus predicted values) for net photosynthesis (P_n) obtained after adjusting the
565 non-rectangular hyperbola (white), the rectangular hyperbola (black) and the exponential (gray) models to the
566 field data of irradiance curves of photosynthesis, when dark respiration (R_d) was estimated by the models, in ten
567 tropical tree species in flooding (right) and non-flooding (left) periods.

568
569 **Figure 2.** Predicted and measured values of the maximum net photosynthesis (P_{nmax} , A-B), dark respiration (R_d ,
570 C-D) estimated by the models and apparent quantum yield (α , E-F) in ten tropical tree species in non-flooding
571 (A, C, E) and flooding (B, D, F) periods.

572
573 **Figure 3.** Residuals for net photosynthesis (P_n) values obtained after adjusting the non-rectangular hyperbola
574 (white), the rectangular hyperbola (black) and the exponential (gray) models to field data on irradiance curves of
575 photosynthesis, when measured dark respiration (R_d) is included in the models, in ten tropical tree species in
576 flooding and non-flooding periods. *The residual value for P_n was 0 at PPFD = 0 $\mu\text{mol m}^{-2} \text{s}^{-1}$ because, in this
577 situation, the estimated R_d is equal the R_d from measured data.

578
579 **Figure 4.** Predicted and measured values of the maximum net photosynthesis (P_{nmax} , A-B), apparent quantum
580 yield (α , C-D) and convexity term (θ) in ten tropical tree species in non-flooding (A, C, E) and flooding (B, D, F)
581 periods. *Dark respiration was not estimated by the models because the measured R_d was added to the models.
582

583

584 **Table 1.** Non-linear photosynthesis-irradiance models

Model number	Description	Model
1	Non-rectangular hyperbola (NRH)	$P_n = \{[(\alpha I + P_{nmax} + R_d) - ((\alpha I + P_{nmax} + R_d)^2 - 4\alpha I \theta (P_{nmax} + R_d))^{0.5}] / 2\theta\} - R_d$
2	Rectangular hyperbola (RH)	$P_n = \alpha I (P_{nmax} + R_d) / [\alpha I + (P_{nmax} + R_d)] - R_d$
3	Exponential (EXP)	$P_n = (P_{nmax} + R_d) \{1 - \exp[-\alpha I / (P_{nmax} + R_d)]\} - R_d$

585

586

587

588 **Table 2.** Statistical indices for accessing the quantitative performance of non-rectangular
589 hyperbola (NRH), rectangular hyperbola (RH) and exponential (EXP) models describing the
590 irradiance response of photosynthesis when dark respiration (R_d) was estimated by the models
591 in ten tropical tree species in the non-flooding period (NFP) and flooding period (FP).

Species	Non-rectangular hyperbola						Rectangular hyperbola						Exponential					
	Non-flooding (NFP)			Flooding (FP)			Non-flooding (NFP)			Flooding (FP)			Non-flooding (NFP)			Flooding (FP)		
	r^2	Au d(%)	R M SE	r^2	Au d(%)	R M SE	r^2	Au d(%)	R M SE	r^2	Au d(%)	R M SE	r^2	Au d(%)	R M SE	r^2	Au d(%)	R M SE
<i>N. amazonum</i>	0.99	27.3	49.6	0.99	22.4	45.0	0.99	16.9	16.9	0.99	17.1	17.1	0.99	12.3	34.3	0.99	9.4	3.3
<i>M. angustifolium</i>	0.99	20.4	45.6	0.99	14.9	35.4	0.00	09.4	09.4	0.99	16.6	16.6	0.99	11.3	36.3	0.99	5.9	6.6
<i>A. discolor</i>	0.99	31.3	59.5	0.99	20.9	48.2	0.99	15.3	15.3	0.99	11.0	11.0	0.99	20.9	48.7	0.99	15.3	39.6
<i>B. lactescens</i>	0.97	28.3	60.5	0.98	21.4	44.0	0.99	30.4	30.4	0.99	13.8	13.8	0.97	24.7	57.4	0.98	16.8	39.2
<i>S. reticulata</i>	0.99	33.7	62.3	0.99	17.6	66.1	0.99	15.4	28.0	0.00	18.0	18.0	0.99	24.9	24.9	0.99	4.5	0.0
<i>G. spruceana</i>	0.99	19.3	40.2	0.99	16.4	35.3	0.99	6.4	3.8	0.99	6.2	4.8	0.99	8.8	6.8	0.99	6.9	0.0
<i>P. excelsa</i>	0.99	19.4	37.7	0.99	12.5	26.8	0.00	07.3	5.6	0.99	24.1	24.1	0.99	10.7	28.0	0.99	3.3	4.4
<i>C. concolor</i>	0.99	26.9	54.1	0.97	17.5	21.9	0.99	8.3	9.9	0.99	4.2	1.9	0.99	8.4	4.2	0.98	12.0	17.7
<i>V. guianensis</i>	0.98	17.1	52.3	0.97	16.2	12.9	0.99	4.4	3.9	0.98	10.2	08.1	0.99	10.3	45.6	0.98	8.1	09.9
<i>V. japurensis</i>	0.98	31.4	58.7	0.97	16.7	15.0	0.99	7.8	7.9	0.99	5.3	2.4	0.98	24.7	54.5	0.98	9.5	10.0
Average	0.99	25.6	0.52	0.98	17.7	0.35	0.99	6.9	0.19	0.99	6.2	0.13	0.99	13.8	0.38	0.99	9.2	0.23

592 r^2 = coefficient of determination; *Aud*(%) = the average of unsigned deviation; *RMSE* = the
593 root mean square of error (*RMSE*).
594

595

596

Table 3. Measured and estimated photosynthesis maxima (P_{nmax}) from three models when dark respiration (R_d) was estimated by the models in ten tropical tree species in two flooding

597

598

periods.

	Measured		Non-rectangular hyperbola				Rectangular hyperbola				Exponential		
	Non-flooding	Flooding	Non-flooding		Flooding		Non-flooding		Flooding		Non-flooding		Flooding
	Mean (min-max)	Mean (min-max)	%	r^2	%	r^2	%	r^2	%	r^2	%	r^2	%
<i>Alseodaphnophloeum</i>	15.1 (11.6-19.3)	14.2 (11.7-17.1)	38.5	0.888	36.1	0.766	16.4	0.995	16.2	0.998	-2.0	0.996	-1.9
<i>Alseodaphnophloeum</i>	11.9 (9.3-15.6)	10.4 (7.5-13.0)	33.7	0.987	29.7	0.508	11.9	0.997	12.2	0.996	-3.5	0.998	-2.3
<i>Alseodaphnophloeum</i>	14.4 (10.1-18.2)	11.6 (6.5-16.9)	70.9	0.473	62.4	0.671	25.8	0.778	22.4	0.940	1.5	0.920	-0.1
<i>Alseodaphnophloeum</i>	10.4 (7.2-13.4)	9.2 (5.9-10.9)	80.5	0.414	55.1	0.641	11.0	0.971	14.2	0.967	-3.2	0.995	-2.0
<i>Alseodaphnophloeum</i>	27.3 (24.8-30.1)	26.6 (21.3-32.4)	43.3	0.754	49.5	0.525	31.1	0.877	36.9	0.945	3.1	0.974	5.2
<i>Alseodaphnophloeum</i>	14.4 (12.0-16.5)	12.0 (10.5-15.3)	34.4	0.982	31.0	0.978	17.1	0.975	15.3	0.997	-1.5	0.993	-1.6
<i>Alseodaphnophloeum</i>	11.1 (9.6-14.3)	9.6 (7.1-12.9)	37.5	0.889	24.6	0.952	14.0	0.985	13.3	0.992	-2.4	0.994	-2.0
<i>Alseodaphnophloeum</i>	22.8 (17.2-27.7)	3.0 (0.1-9.3)	45.4	0.779	29.5	0.949	27.4	0.898	7.6	0.998	1.9	0.970	-6.8
<i>Alseodaphnophloeum</i>	11.6 (7.7-16.1)	1.5 (0.8-2.5)	43.2	0.671	20.7	0.818	16.3	0.861	10.0	0.972	-0.5	0.860	-2.7
<i>Alseodaphnophloeum</i>	11.1 (7.8-13.1)	2.1 (0.0-4.9)	59.0	0.639	7.3	0.988	16.6	0.876	5.2	0.998	-1.4	0.907	-4.9
<i>Alseodaphnophloeum</i>	15.0 (7.2-30.1)	10.0 (0.0-32.4)	48.3	0.861	41.0	0.958	20.8	0.980	20.9	0.986	-0.2	0.992	-0.1

599

Mean (min-max) of ten repetitions for each species in the non-flooding and flooding periods.

600

The percentages (%) represent changes (positive or negative relative to measured values) that

601

occurred in P_{nmax} estimated by the NRH, RH and EXP models. r^2 = coefficient of

602

determination

603

604

605 **Table 4.** Measured and estimated dark respiration (R_d) by three models in ten tropical tree
 606 species in two flooding periods.

	Measured		Non-rectangular hyperbola				Rectangular hyperbola				Exponential		
	Non-flooding	Flooding	Non-flooding		Flooding		Non-flooding		Flooding		Non-flooding	Flooding	
	Mean (min-max)	Mean (min-max)	%	r^2	%	r^2	%	r^2	%	r^2	%	r^2	
<i>num</i>	1.44 (0.77-2.51)	1.37 (0.95-2.79)	-62.6	0.916	-60.5	0.955	16.2	0.890	18.4	0.893	-27.3	0.852	-23.8
<i>ifolium</i>	0.61 (0.43-0.88)	0.80 (0.43-1.04)	-128.9	0.412	-85.2	0.829	26.1	0.882	25.7	0.780	-56.1	0.240	-26.3
<i>r</i>	1.73 (0.86-2.27)	1.84 (1.19-2.69)	-60.2	0.891	-50.2	0.878	-9.0	0.680	-6.1	0.815	-37.9	0.777	-32.8
<i>ens</i>	0.74 (0.45-1.17)	0.83 (0.54-1.17)	-150.3	0.328	-104.7	0.655	-36.5	0.339	-20.5	0.509	-122.3	0.219	-74.8
<i>ata</i>	1.63 (0.79-2.18)	2.04 (1.32-2.67)	-67.4	0.903	-48.5	0.823	16.9	0.904	12.6	0.540	-21.6	0.880	-13.8
<i>ana</i>	1.00 (0.59-1.45)	0.78 (0.61-1.06)	-75.2	0.869	-86.5	0.761	29.1	0.969	32.4	0.833	-26.3	0.939	-22.4
<i>r</i>	0.56 (0.30-1.03)	0.72 (0.47-1.43)	-130.3	0.759	-67.6	0.252	20.4	0.810	42.8	0.714	-64.7	0.731	-9.0
<i>or</i>	1.50 (0.99-2.49)	0.97 (0.40-1.69)	-68.6	0.612	-38.4	0.682	15.7	0.601	1.7	0.921	-26.3	0.561	-13.8
<i>nsis</i>	1.08 (0.77-1.48)	0.88 (0.45-1.20)	-77.1	0.488	-25.0	0.963	10.0	0.664	5.5	0.907	-39.1	0.518	-2.6
<i>nsis</i>	1.21 (0.70-2.04)	0.68 (0.40-1.00)	-92.1	0.802	-45.8	0.637	-26.7	0.706	3.4	0.963	-71.6	0.730	-8.7
<i>s</i>	1.15 (0.30-2.51)	1.09 (0.40-2.79)	-81.7	0.770	-58.3	0.692	5.8	0.749	9.9	0.839	-43.1	0.707	-23.0

607 Mean (min-max) of ten repetitions for each species in the non-flooding and flooding periods.

608 The percentages (%) represent changes (positive or negative relative to measured values) that
 609 occurred in R_d estimated by the NRH, RH and EXP models. r^2 = coefficient of determination.

610

611
612 **Table 5.** Measured values (including points of Kok-effect region) and estimated apparent
613 quantum yield (α) by initial slope excluding points of Kok-effect region, and by the RH and
614 EXP models when dark respiration (R_d) was estimated by the models in ten tropical tree
615 species in two flooding periods.

	Measured		Estimated excluding kok effect				Rectangular hyperbola				Exponential		
	Non-flooding	Flooding	Non-flooding		Flooding		Non-flooding		Flooding		Non-flooding		Flooding
	Mean (min-max)	Mean (min-max)	%	r^2	%	r^2	%	r^2	%	r^2	%	r^2	%
<i>um</i>	0.054 (0.047-0.061)	0.052 (0.047-0.054)	-6.0	0.952	-6.0	0.916	53.8	0.209	57.8	0.166	2.8	0.247	5.9
<i>folium</i>	0.048 (0.043-0.053)	0.046 (0.038-0.053)	-6.5	0.918	-8.3	0.988	61.9	0.009	79.5	0.670	6.4	0.001	19.7
<i>r</i>	0.047 (0.036-0.055)	0.041 (0.030-0.052)	-9.6	0.952	-12.0	0.930	31.6	0.885	37.0	0.773	-9.5	0.862	-9.5
<i>ens</i>	0.043 (0.033-0.054)	0.036 (0.027-0.045)	-9.4	0.974	-12.3	0.926	24.6	0.034	36.2	0.818	-24.7	0.178	-13.8
<i>ata</i>	0.058 (0.053-0.068)	0.052 (0.045-0.059)	-7.0	0.626	-3.9	0.948	35.8	0.638	30.4	0.509	2.7	0.451	1.4
<i>ana</i>	0.049 (0.043-0.067)	0.044 (0.038-0.048)	-5.3	0.982	-6.7	0.884	56.5	0.946	65.1	0.580	6.0	0.952	12.9
<i>e</i>	0.041 (0.034-0.052)	0.041 (0.026-0.057)	-7.5	0.989	-4.6	0.975	54.4	0.832	79.4	0.808	1.2	0.786	20.6
<i>or</i>	0.056 (0.047-0.066)	0.020 (0.007-0.041)	-6.6	0.457	-15.6	0.993	38.2	0.317	117.5	0.774	0.4	0.304	38.7
<i>nsis</i>	0.049 (0.038-0.057)	0.017 (0.012-0.021)	-7.4	0.902	-13.9	0.781	56.5	0.637	184.2	0.013	2.9	0.509	73.5
<i>nsis</i>	0.041 (0.033-0.049)	0.018 (0.005-0.034)	-12.2	0.882	-22.6	0.994	21.7	0.665	147.5	0.753	-15.2	0.567	51.2
<i>s</i>	0.049 (0.033-0.068)	0.037 (0.005-0.059)	-7.6	0.923	-8.9	0.986	43.8	0.572	70.0	0.607	-1.2	0.647	13.8

616 Mean (min-max) of ten repetitions for each species in the non-flooding and flooding periods.
617 The percentages (%) represent changes (positive or negative relative to measured values) that
618 occurred in R_d estimated by the NRH, RH and EXP models. r^2 = coefficient of determination.
619

620
621
622
623
624
625

Table 6. Statistical indices for accessing the quantitative performance of non-rectangular hyperbola (NRH), rectangular hyperbola (RH) and exponential (EXP) models describing the irradiance response of photosynthesis, when measured dark respiration (R_d) was added in the models, in ten tropical species in non flooding (NFP) and flooding period (FP).

Species	Non-rectangular hyperbola						Rectangular hyperbola						Exponential						
	Non-flooding (NFP)			Flooding (FP)			Non-flooding (NFP)			Flooding (FP)			Non-flooding (NFP)			Flooding (FP)			
	Aud (%)	R MS E	r ²	Aud (%)	R MS E	r ²	Aud (%)	R MS E	r ²	Aud (%)	R MS E	r ²	Aud (%)	R MS E	r ²	Aud (%)	R MS E	R MS E	
<i>N. amazonum</i>	0.9	40.87	0.70	0.9	35.88	0.64	0.9	12.99	0.18	0.9	12.99	0.20	0.9	15.96	0.38	0.9	12.96	0.03	0.344
<i>M. angustifolium</i>	0.9	15.81	0.62	0.9	15.84	0.51	0.9	3.699	0.4	0.9	5.898	0.6	0.9	6.292	0.7	0.9	6.296	4.6	0.60
<i>A. discolor</i>	0.9	55.77	0.87	0.9	40.76	0.74	0.9	10.99	0.17	0.9	8.099	0.6	0.9	35.89	0.62	0.9	88.7	25.7	0.520
<i>B. lactescens</i>	0.9	23.54	0.82	0.9	27.67	0.64	0.9	5.299	0.5	0.9	5.098	0.9	0.9	15.68	0.68	0.9	82.9	3.75	0.475
<i>S. reticulata</i>	0.9	52.93	0.92	0.9	27.93	0.90	0.9	4.399	0.00	1.0	6.900	0.31	0.9	21.99	0.31	0.9	99.7.4	0.9	0.309
<i>G. spruceana</i>	0.9	19.90	0.58	0.9	16.88	0.51	0.9	9.098	0.2	0.9	6.498	0.20	0.9	5.898	0.27	0.9	97.5.3	0.9	0.244
<i>P. excelsa</i>	0.9	15.84	0.54	0.9	13.90	0.37	1.0	2.700	0.08	0.9	9.895	0.26	0.9	7.294	0.32	0.9	98.2.4	0.9	0.166
<i>C. concolor</i>	0.9	41.92	0.83	0.9	34.52	0.29	0.9	3.899	0.26	0.9	4.099	0.05	0.9	17.99	0.33	0.9	80.7	14.88	0.188
<i>V. guianensis</i>	0.9	21.76	0.69	0.9	27.59	0.15	0.9	4.699	0.13	0.9	10.88	0.08	0.9	9.988	0.49	0.9	83.7.7	0.9	0.099
<i>V. japurensis</i>	0.9	46.62	0.83	0.9	36.44	0.20	0.9	11.0	0.28	0.9	5.499	0.03	0.9	31.76	0.66	0.9	86.0	11.03	0.103
Average	0.979	33.3	0.745	0.974	27.6	0.499	0.998	6.7	0.210	0.997	7.4	0.153	0.990	16.5	0.448	0.991	10.8	0.271	

626 r^2 = coefficient of determination; Aud(%) = the average of unsigned deviation; RMSE = the
627 root mean square of error.
628

629
630
631

Table 7. Estimated photosynthesis maxima (P_{nmax}) from three models when measured dark respiration (R_d) was added to the models in ten tropical tree species in two flooding periods.

Species	Non-rectangular hyperbola				Rectangular hyperbola				Exponential			
	Non-flooding		Flooding		Non-flooding		Flooding		Non-flooding		Flooding	
	%	r^2	%	r^2	%	r^2	%	r^2	%	r^2	%	r^2
<i>N. amazonum</i>	22.0	0.962	20.4	0.930	17.2	0.994	17.0	0.998	-2.8	0.993	-2.6	0.983
<i>M. angustifolium</i>	17.0	0.993	13.4	0.869	12.4	0.997	12.5	0.993	-4.2	0.997	-3.1	0.984
<i>A. discolor</i>	42.5	0.622	32.2	0.912	23.1	0.886	21.3	0.951	-1.1	0.960	-2.5	0.985
<i>B. lactescens</i>	26.9	0.915	26.5	0.816	9.1	0.951	12.5	0.983	-7.6	0.954	-5.3	0.990
<i>S. reticulata</i>	32.1	0.805	37.5	0.711	32.3	0.833	38.0	0.968	2.5	0.957	4.5	0.992
<i>G. spruceana</i>	21.1	0.989	17.9	0.992	18.2	0.973	16.3	0.996	-1.9	0.991	-2.2	0.997
<i>P. excelsa</i>	19.7	0.964	12.8	0.967	14.4	0.984	14.3	0.990	-3.3	0.991	-2.2	0.988
<i>C. concolor</i>	32.2	0.814	33.2	0.977	28.3	0.902	7.6	0.997	1.2	0.968	-7.7	0.997
<i>V. guianensis</i>	20.9	0.824	7.4	0.842	16.5	0.852	10.3	0.970	-1.7	0.849	-3.0	0.977
<i>V. japurensis</i>	32.1	0.416	27.8	0.935	12.9	0.967	5.3	0.998	-6.0	0.990	-5.2	0.999
All species	27.7	0.945	34.3	0.972	20.8	0.985	21.2	0.986	-1.6	0.993	-1.1	0.997

632 * See Mean (min-max) of measured P_{nmax} in **Table 3**
 633 ** The percentages (%) represent changes (positive or negative relative to measured values)
 634 that occurred in P_{nmax} estimated by the NRH, RH and EXP models. r^2 = coefficient of
 635 determination.
 636

637
 638
 639
 640

Table 8. Estimated apparent quantum yield (α) from the RH and EXP models when measured dark respiration (R_d) was added to the models, in ten tropical tree species in two flooding periods.

Species	Rectangular hyperbola				Exponential			
	Non-flooding		Flooding		Non-flooding		Flooding	
	%	r^2	%	r^2	%	r^2	%	r^2
<i>N. amazonum</i>	45.6	0.314	47.9	0.256	11.8	0.380	13.8	0.273
<i>M. angustifolium</i>	53.8	0.042	67.1	0.630	16.9	0.055	26.0	0.678
<i>A. discolor</i>	33.5	0.884	42.3	0.706	2.8	0.892	9.4	0.741
<i>B. lactescens</i>	39.7	0.415	45.9	0.793	4.4	0.389	9.6	0.771
<i>S. reticulata</i>	30.7	0.881	25.4	0.696	7.0	0.834	4.6	0.706
<i>G. spruceana</i>	45.5	0.940	53.2	0.591	12.5	0.940	17.4	0.666
<i>P. excelsa</i>	48.4	0.917	61.8	0.903	13.0	0.927	23.6	0.913
<i>C. concolor</i>	33.1	0.578	114.7	0.820	6.3	0.633	53.0	0.907
<i>V. guianensis</i>	52.4	0.848	169.1	0.003	15.8	0.859	77.2	0.109
<i>V. japurensis</i>	37.0	0.828	142.6	0.874	2.3	0.744	59.1	0.928
All species	41.7	0.696	64.7	0.653	9.4	0.773	23.6	0.808

641
 642
 643
 644

* See Mean (min-max) of measured α in **Table 5**

** The percentages (%) represent changes (positive or negative relative to measured values) that occurred in P_{nmax} estimated by the RH and EXP models. r^2 = coefficient of determination.

645
646
647

Table 9. Estimated convexity term (θ) by non-rectangular hyperbola when dark respiration (R_d) was estimated by the models, in ten tropical tree species in two flooding periods.

Species	Measured		Non-rectangular hyperbola			
	Non-flooding	Flooding	Non-flooding		Flooding	
	Mean (min-max)	Mean (min-max)	%	r^2	%	r^2
<i>N. amazonum</i>	0.862 (0.824-0.909)	0.869 (0.815-0.897)	5.4	0.783	5.1	0.903
<i>M. angustifolium</i>	0.867 (0.827-0.906)	0.890 (0.719-0.948)	5.9	0.973	5.2	0.960
<i>A. discolor</i>	0.813 (0.713-0.922)	0.816 (0.652-0.897)	7.1	0.947	9.2	0.302
<i>B. lactescens</i>	0.761 (0.610-0.903)	0.792 (0.578-0.893)	15.3	0.717	12.1	0.515
<i>S. reticulata</i>	0.865 (0.839-0.883)	0.860 (0.799-0.901)	3.2	0.720	3.1	0.994
<i>G. spruceana</i>	0.872 (0.856-0.887)	0.881 (0.864-0.918)	4.5	0.660	4.6	0.820
<i>P. excelsa</i>	0.857 (0.831-0.888)	0.904 (0.860-0.992)	6.2	0.897	4.1	0.971
<i>C. concolor</i>	0.858 (0.822-0.889)	0.908 (0.776-0.999)	3.9	0.679	1.5	0.611
<i>V. guianensis</i>	0.858 (0.769-0.954)	0.950 (0.811-0.994)	6.9	0.894	2.9	0.917
<i>V. japurensis</i>	0.767 (0.610-0.852)	0.966 (0.906-0.990)	13.5	0.864	3.3	0.105
<i>All species</i>	0.838 (0.610-0.954)	0.884 (0.578-0.999)	7.0	0.7334	4.5	0.724

648 Mean (min-max) of ten repetitions for each species in non-flooding and flooding periods. The
649 percentages (%) represent changes (positive or negative relative to measured values) that
650 occurred in θ estimated by the NRH model when R_d was added to the model. r^2 = coefficient
651 of determination

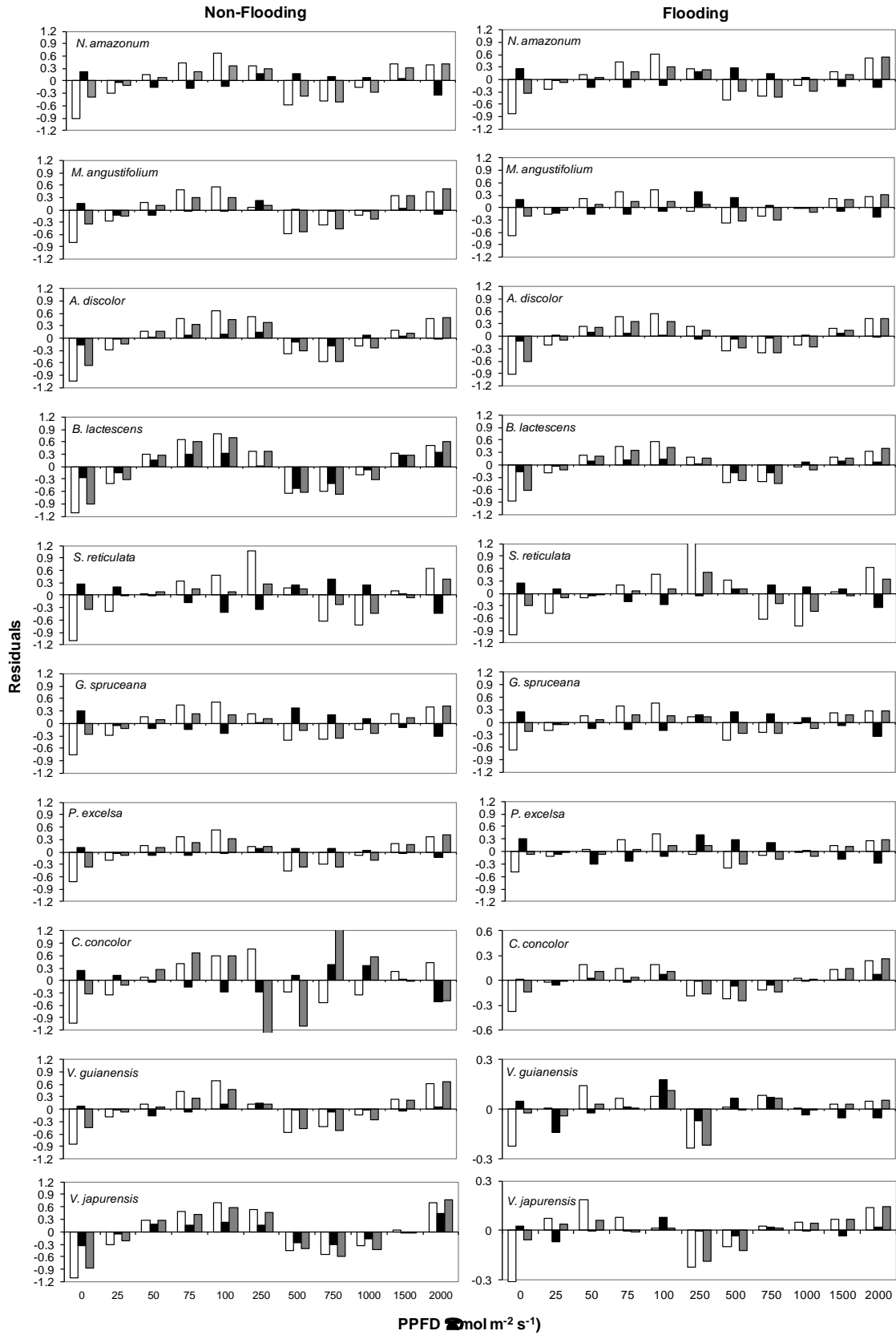


Figure 1

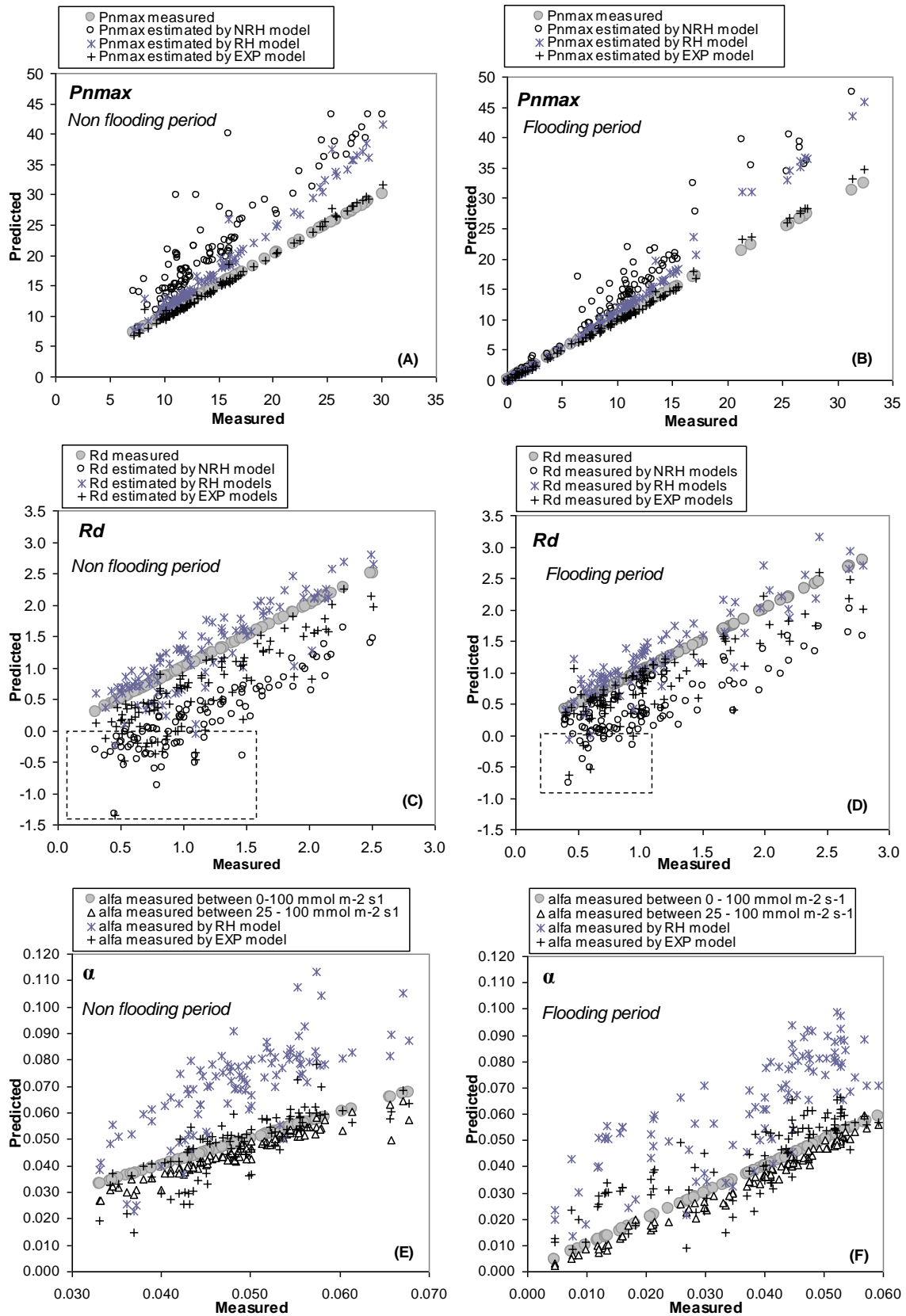


Figure 2

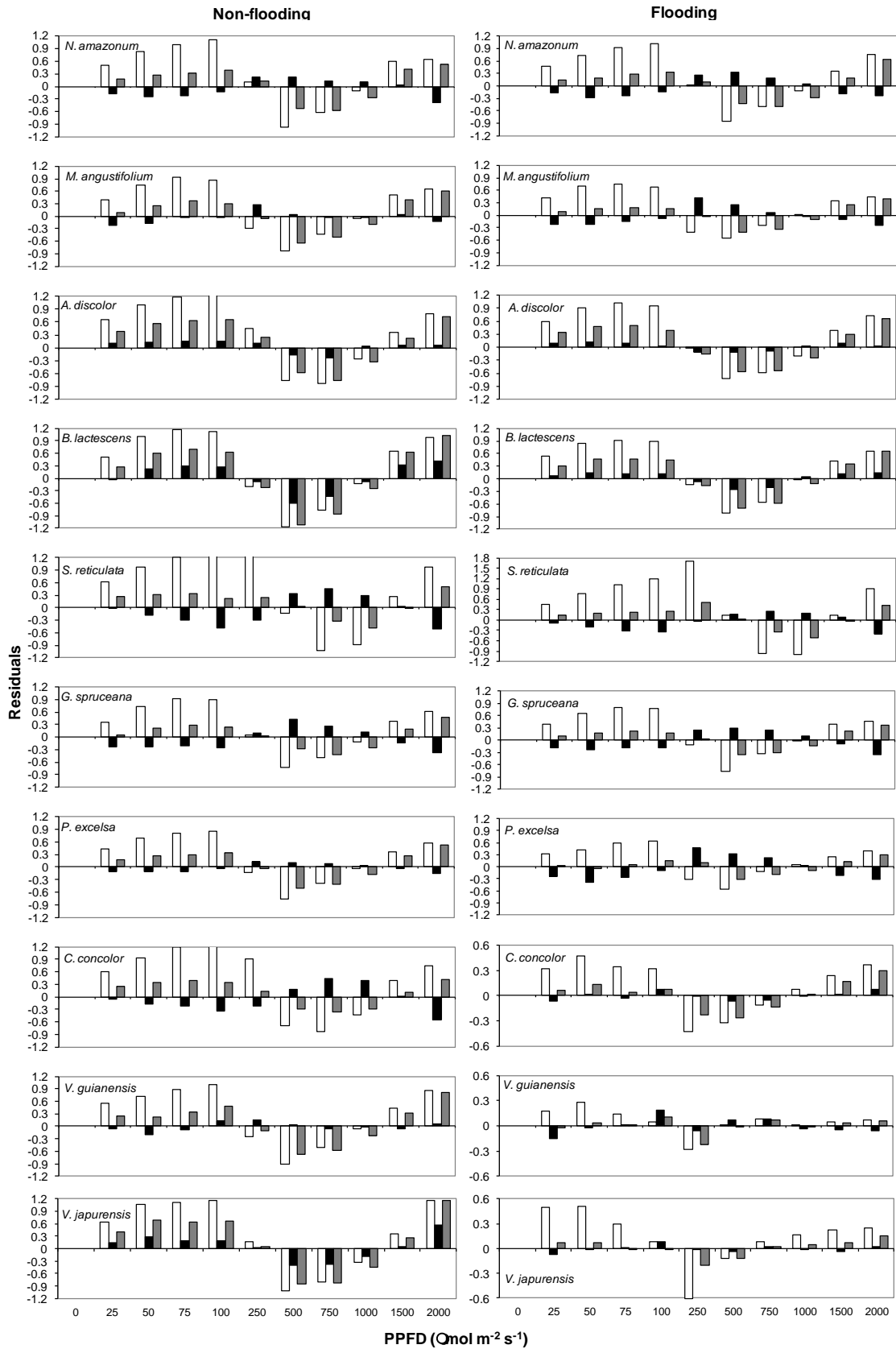


Figure 3

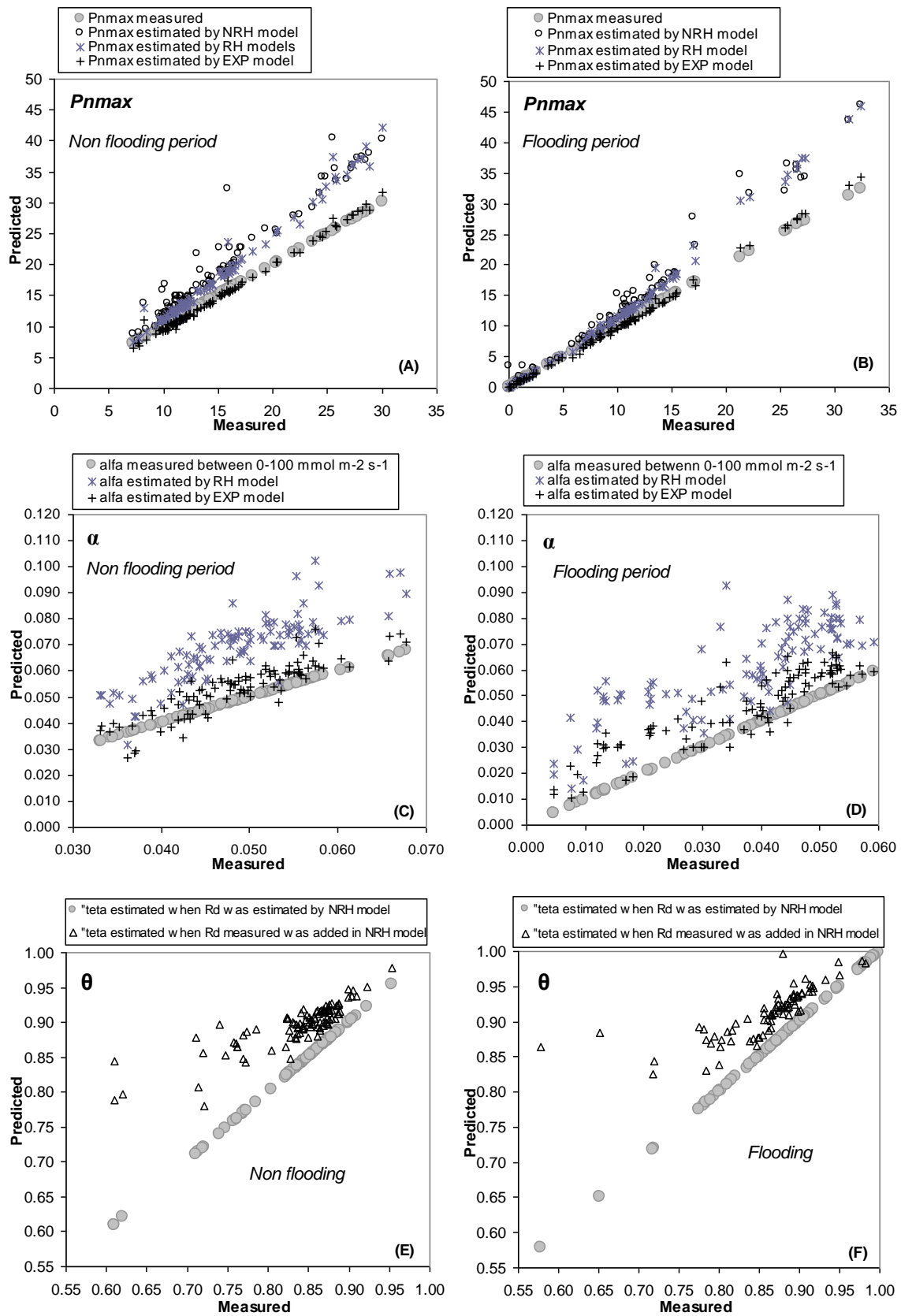


Figure 4